

## In-situ Calibration of the Hydroperoxyl Radical Using an Immobilized TiO<sub>2</sub> Photocatalyst in the Atmosphere

Bum Gun Kwon<sup>a</sup>

Environmental & Whole Information System (E&WIS), #804 Byuksan Digital Valley III 212-13, Guro-3-dong Guro-gu, Seoul 152-848, Korea. E-mail: kwonbg0@daum.net

Received March 18, 2007

The present study is the first report of utilizing TiO<sub>2</sub> photocatalyst to analytically calibrate the hydroperoxyl radical (HO<sub>2</sub>·). An in-situ calibration method of HO<sub>2</sub>· is proposed for air monitoring by using an 2-methyl-6-(*p*-methoxyphenyl)-3,7-dihydroimidazo-[1,2-*a*]pyrazin-3-one (MCLA)-chemiluminescence (CL) technique. In this method, HO<sub>2</sub>· (pK<sub>a</sub> = 4.80) is produced by the ultraviolet (UV) photolysis of immobilized TiO<sub>2</sub> using a constant flow rate of air equilibrated water, in which HO<sub>2</sub>· is controlled by using various lengths of knotted tubing reactor (KTR). The principle of the proposed calibration is based on the experimentally determined half-life (t<sub>1/2</sub>) of HO<sub>2</sub>· and its empirically observed pH-dependent rate constant, *k*<sub>obs</sub>, at a given pH. The concentration of HO<sub>2</sub>/O<sub>2</sub><sup>-</sup> is increased as pH increases. This pH dependence is due to the different disproportionative reactivities between HO<sub>2</sub>/O<sub>2</sub><sup>-</sup> and HO<sub>2</sub>·/O<sub>2</sub><sup>-</sup>. Experimental results indicate the practical feasibility of the approach, producing very promising method.

**Key Words :** Hydroperoxyl radical, *In-situ* calibration, TiO<sub>2</sub>, Kinetic method

### Introduction

The quantitative analysis of trace hydroperoxyl radicals (HO<sub>2</sub>·) in the atmosphere is crucially important in studying the formation of photochemical smog through its reaction with NO to yield NO<sub>2</sub>, which is photolyzed in the troposphere to generate O<sub>3</sub>.<sup>1-11</sup> Conventional methods of quantifying HO<sub>2</sub>· include laser-induced fluorescence (LIF),<sup>5</sup> fluorescence assay with gas expansion (FAGE),<sup>11,12</sup> electron spin resonance spectroscopy coupled with matrix isolation (MIESR),<sup>3,11</sup> chemical amplifier technique (CAT) by luminol CL,<sup>1-3,7</sup> and peroxy radical chemical ionization mass spectroscopy (PerCIMS).<sup>11</sup> Each of these methods has certain advantages and limitations in terms of accuracy, sensitivity, special material and time demands, and environmental risks, as follows. The LIF method is highly specific for the hydroxyl radical (·OH) and exhibits a 0.004 pptv detection limit with a signal-noise ratio (S/N) = 2 in 30 s.<sup>5</sup> HO<sub>2</sub>· can also be measured after reaction with excess NO, followed by detection of the resulting ·OH by LIF at 308 nm.<sup>5,10</sup> The FAGE method is an indirect measurement, as HO<sub>2</sub>· must first be converted to the hydroxyl radical through the reaction (HO<sub>2</sub>· + NO) prior to spectroscopic detection.<sup>11,12</sup> Since sufficient NO must be added to ensure rapid conversion in the short reaction time between NO addition and the ·OH excitation reaction (typically ~1 ms in the fast flows employed),<sup>11</sup> however, there is a competing reaction (·OH + NO). Thus, it is not possible to convert all of the HO<sub>2</sub>· into the hydroxyl radical. The MIESR method allows for direct measurement of peroxy radicals (RO<sub>2</sub>·) including HO<sub>2</sub>·; however, the procedures involved with this

method are characterized by a number of limitations.<sup>3,11</sup> For example, this method requires freezing ambient air in liquid nitrogen (77 K) in a vacuum chamber and using a numerical fitting procedure to determine the concentration of HO<sub>2</sub>·. Moreover, since on some occasions exceedingly high apparent RO<sub>2</sub>· signals have been observed in MIESR, further work is needed to identify HO<sub>2</sub>·.<sup>10</sup> With CAT, using luminol, the CL is related to the modulation in the NO<sub>2</sub> signal by a calibration factor equal to a combination of detector sensitivity and chain length of the chemical amplifier, giving an estimated detection limit of about 1 pptv in air.<sup>3</sup> However, the accuracy of this technique is rather poor, due to sensitivity of the chain length to conditions in the chemical amplifier and to potential interferences such as peroxyacetyl nitrate (PAN) and peroxyoxynitric acid, which decompose to form radicals in the system.<sup>3</sup> The PerCIMS technique was developed to measure tropospheric HO<sub>2</sub>· and RO<sub>2</sub>·.<sup>11</sup> For this measurement, excess NO is added to produce ·OH upon reaction with peroxy radicals. The hydroxyl radicals react rapidly with added isotopically labeled SO<sub>2</sub>, thus imposing radioactive hazard. The PerCIMS technique has excellent sensitivity and may be able to discriminate between HO<sub>2</sub>· and RO<sub>2</sub>· by controlling the concentration of added NO and SO<sub>2</sub>.<sup>3,11</sup>

All the aforementioned methods for measuring HO<sub>2</sub>· require calibration to determine the signal observed while sampling a known HO<sub>2</sub>· concentration.<sup>11</sup> Although it is possible, in principle, to measure the sensitivity of a given field instrument, the result is unreliable, as many assumptions need to be made about instrumental parameters, some of which may vary with time.<sup>11,13</sup> For example, even though the vacuum-ultraviolet photolysis of water vapor using a pen-ray mercury lamp has been widely used as a calibration method, it is highly desirable to perform this calibration in moist air to ensure that the conditions are very similar to

<sup>a</sup>Present address: Biofilm Engineering Laboratory, School of Chemical Engineering, College of Engineering, Seoul National University, Seoul 151-742, Korea

those encountered during ambient sampling.<sup>3</sup> Thus, water dependence to calibrate  $\text{HO}_2\cdot$  concentration must be known, because  $\text{H}_2\text{O}$  content is quite variable in the atmosphere.

Recently, a flow injection analysis with MCLA-based CL as a specific  $\text{HO}_2\cdot$  detector using wet technique has been proposed, which is based on the CL reaction between  $\text{HO}_2\cdot$  (aq) and MCLA as a synthetic analogue of the luciferin.<sup>10</sup> In this method, known quantities of  $\text{HO}_2\cdot$  (aq) in aqueous solution for calibration standards are produced from  $^{60}\text{Co}$ -radiolysis. However,  $\text{HO}_2\cdot$  generation utilizing  $^{60}\text{Co}$ -radiolysis has required fairly specialized equipment because of the constraints imposed by its instrument design. Another difficulty in field is the performance of an accurate calibration technique due to short half-life of  $\text{HO}_2\cdot$ . For example,  $\text{HO}_2\cdot$  rapidly disappears in acidic solutions and at room temperature.<sup>14,15</sup> Importantly, all the aforementioned methods are still under development<sup>10</sup> and requires in-situ field calibration method. For this reason, the present work aims at developing an *in-situ* calibration method that is simple, fast, and inexpensive while overcoming many other limitations of the present methods.

In this work, we present a method for calibrating  $\text{HO}_2\cdot$  using a wet technique based on the in-situ  $\text{HO}_2\cdot$ -generating technique and experimentally determined half-life ( $t_{1/2}$ ) method. This novel method involves the  $\text{TiO}_2$  photocatalyst as an in-situ radical generator, followed by the separation of  $\text{HO}_2\cdot$  from various reactive species generated through the photolysis of a coil-quartz tube immobilized by  $\text{TiO}_2$  particles. The separated  $\text{HO}_2\cdot$  is then detected using an MCLA-based CL technique, and  $\text{HO}_2\cdot$  is quantified using a simple formula. Uniquely, the calibration method in this study does not require the introduction of known amounts of  $\text{HO}_2\cdot$  into the detector as it uses the probe as an internal standard. For a field application, the traditional calibration methods such as internal and external calibration are not appropriate choices; in some cases, they are not applicable. A new calibration method that can fulfill the demands of a field analysis is introduced in this paper. The developed method is simple, quantitative, fast, and highly sensitive.

## Experimental Section

**Materials.**  $\text{TiO}_2$  particles (Aldrich, 99+%), MCLA (Fluka,  $\geq 98.5\%$ ), ethanol (Merck, 99.8%), sodium hydroxide (GFS Chemicals, 99.999%), and hydrochloric acid (Sigma Co., 99.999%) were used without further purification. The CL reagent was a 12  $\mu\text{M}$  MCLA solution in 1:100 (v/v) ethanol/ $\text{H}_2\text{O}$ , adjusted to pH 2.5 with HCl.<sup>10</sup> The pH-controlled buffer solutions were adjusted to a range between 5.6 and 11 with a borate buffer and NaOH. All solutions were made with high purity deionized water from the Younglin ultra-purification system ( $>18 \text{ M}\Omega \text{ cm}$ ).

**Preparation of Coil-quartz Tube Doped by  $\text{TiO}_2$  Particles.**  $\text{TiO}_2$  particles were immobilized on the inner surface of a coil-quartz tube (inner diameter 2 mm  $\times$  length 900 mm; inner surface area  $\approx 2,800 \text{ mm}^2$ ). The coil-quartz tube was pre-cleaned using 1% nitric acid and washed with DI water

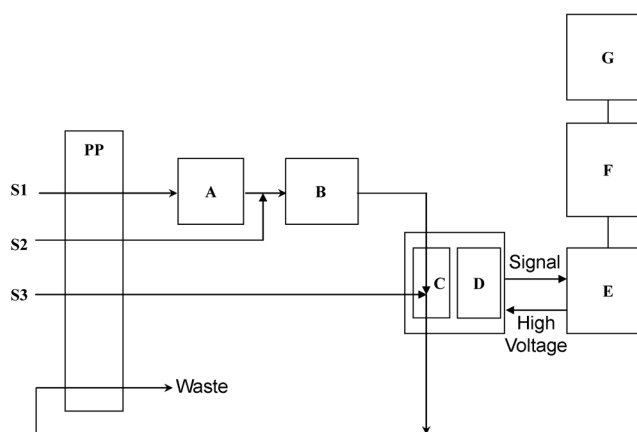


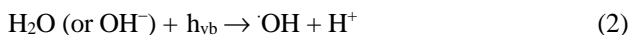
**Figure 1.** Schematic diagram and calibration equipment for measuring  $\text{HO}_2\cdot/\text{O}_2\cdot^-$ . PP, peristaltic pump; A, immobilized  $\text{TiO}_2$  quartz reactor; B, knotted tubing reactors (KTR); C, spiral quartz cell; D, PMT detector; E, Amplifier; F, A/D converter; PC, computer; S1, pure DW; S2, pH-controlled buffer; S3, chemiluminescent reagent solution as MCLA.

by pumping for 2 hr at 1.00 mL/min. 300 mg  $\text{TiO}_2$  particles were added to 3 mL methanol, and stirred with a magnetic stirrer. A 0.3 mL  $\text{TiO}_2$  suspension was gradually poured into the coil-quartz tube and then dried at 40  $^\circ\text{C}$ . This process was repeated ten times to achieve an even coating. The tube was subsequently calcined in a furnace at 600  $^\circ\text{C}$  for 3 hr, and then was cooled to room temperature in air.<sup>16</sup>

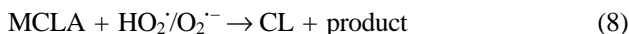
**Apparatus and Procedure for  $\text{HO}_2\cdot$  Determination.** The apparatus set-up for  $\text{HO}_2\cdot$  detection is shown in Figure 1. A carrier solution (S1, 1.0 mL/min), a pH-controlled buffer solution (S2, 0.2 mL/min), and a CL reagent solution (S3, 1.2 mL/min) including MCLA were delivered by using a peristaltic pump (PP, Ismatec Co.) with PTFE tubing (Cole-Palmer, i.d. 0.8 mm). The solution S1 was composed of air-equilibrated water containing dissolved oxygen and was photocatalyzed using a coil-quartz tube (A) doped by  $\text{TiO}_2$  particles, and equipped with a 4-W low pressure Hg lamp ( $\lambda_{\text{max}} = 254 \text{ nm}$ ; Sankyo Denki Co., Japan). The  $\text{HO}_2\cdot$  solution produced from the photolysis using the coil-quartz tube doped by  $\text{TiO}_2$  particles was mixed with a pH-controlled buffer and then was passed through different lengths (0 m, 1 m, 2 m, 3 m, and 4 m, respectively) of a knotted tube reactor (KTR, B), which was able to control the concentration of  $\text{HO}_2\cdot$ . Then,  $\text{HO}_2\cdot$  was detected using MCLA as a specific probe in the fabricated CL detector (D), which had a spiral reaction cell (C) that permitted reagents to mix directly in front of a Hamamatsu R-374 photomultiplier tube (PMT). The CL signal was transferred to a data acquisition system, Auto-chrowin (Younglin, Korea) consisting of a signal amplifier (E), an analog-to-digital converter (A/D, F), and a personal computer (G).

## Results and Discussion

**Reaction Scheme.** The formation of  $\text{HO}_2\cdot$  in a  $\text{TiO}_2$  photolysis is well-known. The basic mechanisms are as follows:<sup>17-27</sup>



In the aqueous phase, the photolysis of hydrated  $\text{TiO}_2$  leads to the formation of a valence band hole ( $h_{\text{vb}}^+$ ) and a conduction band electron ( $e_{\text{cb}}^-$ ) in reaction 1. The hydroxyl radical ( $\cdot\text{OH}$ ) is produced from  $\text{H}_2\text{O}$  (or  $\text{OH}^-$ ) on the  $\text{TiO}_2$  surface by trapping an  $h_{\text{vb}}^+$  (reaction 2). Subsequently, the oxygen molecules adsorbed on the surface of air-saturated  $\text{TiO}_2$  act as electron scavengers and combine with  $e_{\text{cb}}^-$  to form  $\text{O}_2^{\cdot-}$  in reaction 3, which is in an acid-base equilibrium [reaction 4;  $\text{p}K_{\text{a}}(\text{HO}_2^{\cdot}) = 4.80$ ].<sup>14</sup> In this study,  $\text{HO}_2^{\cdot}/\text{O}_2^{\cdot-}$  reacts with the MCLA (reaction 8, *ref.* 25, 28-30) added after the end of the coil-quartz tube as shown in Figure 1.



**Reaction Conditions.** In order to determine the concentration of  $\text{HO}_2^{\cdot}/\text{O}_2^{\cdot-}$ ,  $\text{HO}_2^{\cdot}/\text{O}_2^{\cdot-}$  should be separated from reactive species such as  $\cdot\text{OH}$  and  $h_{\text{vb}}^+$ . This is accomplished by immobilizing  $\text{TiO}_2$  particles onto coil-quartz tube. During illumination,  $\cdot\text{OH}$  and  $h_{\text{vb}}^+$  are present just within the coil-quartz tube due to their short life-times (in the picosecond to millisecond range),<sup>22-24</sup> and thus they can hardly exist in the KTR. In contrast, the life-time of  $\text{HO}_2^{\cdot}/\text{O}_2^{\cdot-}$  is relatively very long, and thus it remains present in the KTR. For example, its half-life ( $t_{1/2}$ ) is approximately 44 seconds at pH 5-6 (*Ref.* 15) and is 2.8 h at pH 11 (*Ref.* 10). Since  $\text{HO}_2^{\cdot}/\text{O}_2^{\cdot-}$  generated from the photolysis of immobilizing  $\text{TiO}_2$  particles exists in the KTR, it is easily separated from reactive species such as  $\cdot\text{OH}$  and  $h_{\text{vb}}^+$ .

Furthermore, since  $\text{H}_2\text{O}_2$  is formed by disproportionation of  $\text{HO}_2^{\cdot}/\text{O}_2^{\cdot-}$  (self-reactions 1-3), this was reported to be potential interference.<sup>10</sup> However, the following experimental results denied this possibility. As shown in Figure 2, the CL intensity is inversely proportional to an increasing length of KTR at pH 5.8 with pure water, indicating that the CL intensity decreases with an increasing reaction time. This

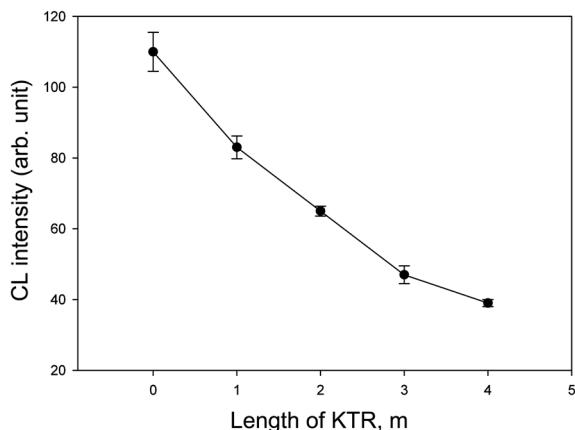


**Figure 2.** Dependence of the CL intensity on increasing the length of KTR:  $[\text{MCLA}] = 12 \mu\text{M}$ ,  $[\text{DO}] = 0.094 \text{ mM}$ ,  $\lambda = 254 \text{ nm}$ , and  $\text{pH} = 5.8$ .

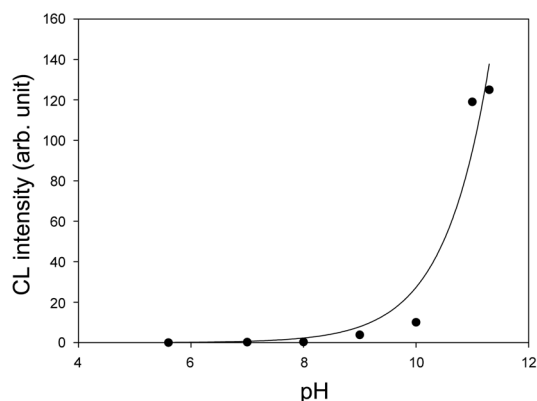


**Figure 3.** Dependence of the background CL intensity on increasing pH:  $[\text{MCLA}] = 12 \mu\text{M}$ ,  $[\text{DO}] = 0.094 \text{ mM}$ ,  $\lambda = 254 \text{ nm}$ , and  $\text{KTR} = 0 \text{ m}$ .

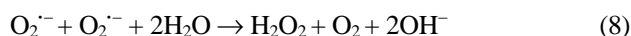
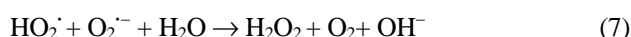
result is due to the  $k_{\text{obs}}$  values on the disproportionation reactions of  $\text{HO}_2^{\cdot}/\text{O}_2^{\cdot-}$  and the pH dependences of the acid-base equilibrium between  $\text{HO}_2^{\cdot}$  and  $\text{O}_2^{\cdot-}$ , which was consistent with the kinetic data by Bielski *et al.*<sup>14</sup> If  $\text{H}_2\text{O}_2$  produces the CL, the CL intensity should not decrease with an increasing reaction time. Hence, the CL originates from the reaction of MCLA with  $\text{HO}_2^{\cdot}/\text{O}_2^{\cdot-}$  generated through the immobilization of  $\text{TiO}_2$  particles. Thus, photocatalytic produced  $\text{HO}_2^{\cdot}/\text{O}_2^{\cdot-}$  can be used for calibration standards.

The working conditions for detection of  $\text{HO}_2^{\cdot}/\text{O}_2^{\cdot-}$  by the CL method using MCLA have been previously described.<sup>10</sup> However, because of the newly fabricated CL detector in this study, the enhanced CL detection system was optimized *via* small modifications. In addition, since the MCLA-based CL emission yields a high background signal at a high pH, it may result in errors as well as a poor detection limit. Thus, the optimum conditions for this detector were reinvestigated for background CL at an alkaline condition, high MCLA concentrations, and flow rate.

The dependence of background CL on various pH conditions was investigated for  $\text{MCLA} = 12 \mu\text{M}$ ,  $\text{KTR} = 0 \text{ m}$ , and flow rate = 1.2 mL/min. In this experiment, the pH levels of the carrier solution were limited to a range of 5.6 (pure water only) to 11 with NaOH. As shown in Figure 3, the intensity of the background CL depends significantly on the pH of the carrier solution. The intensities of the background CL are almost invariable in lower pH ranges ( $\text{pH} < 9$ ), whereas they gradually increase in the pH range of 9-10 and rapidly increase thereafter. The CL emission of MCLA has been generated from air oxidation of MCLA at a high pH, producing CL identical to that from  $\text{HO}_2^{\cdot}/\text{O}_2^{\cdot-}$ .<sup>10</sup> Thus, carrier solutions were adjusted to below pH 9 to prevent a signal of background CL from a high pH. The dependence of the CL on MCLA concentration was investigated for  $\text{pH} = 8$ ,  $\text{KTR} = 0 \text{ m}$ , and flow rate = 1.2 mL/min. In this experiment, the concentration range of MCLA producing the largest responses was from  $8 \mu\text{M}$  to  $12 \mu\text{M}$  (data not shown). In addition, the dependence of the CL on the flow rate was investigated for  $\text{pH} = 8$ ,  $\text{KTR} = 0 \text{ m}$ , and  $[\text{MCLA}] = 1.2 \mu\text{M}$ . Our result showed that the proper flow rates of a carrier solution and an

MCLA solution were respective 1.2 mL/min (data not shown). These results were observed to be similar to those of Zheng *et al.*<sup>10</sup> Finally, all experimental conditions for the CL detection of the  $\text{HO}_2\cdot/\text{O}_2^{\cdot-}$  were adjusted to below pH 9 by using a borate buffer and NaOH,  $[\text{MCLA}] = 1.2 \mu\text{M}$ , and flow rate = 1.2 mL/min.

**Calibration for  $\text{HO}_2\cdot$ .** The basic principle of calibration employed in this work is described in detail in a previous study.<sup>15</sup> In the absence of additives,  $\text{HO}_2\cdot/\text{O}_2^{\cdot-}$  is disproportionated by self-reactions 6-8:<sup>14</sup>



where  $k_6 = (8.3 \pm 0.7) \times 10^5 \text{ M}^{-1} \text{ s}^{-1}$ ,  $k_7 = (9.76 \pm 0.6) \times 10^7 \text{ M}^{-1} \text{ s}^{-1}$ ,  $k_8 < 0.3 \text{ M}^{-1} \text{ s}^{-1}$ .<sup>14</sup> If reaction 8 is ignored, the empirically observed pH-dependent rate constant,  $k_{\text{obs}}$ , at a given pH is

$$k_{\text{obs}} = \{k_6 + k_7(K_{\text{HO}_2}/[\text{H}^+])\}/(1 + K_{\text{HO}_2}/[\text{H}^+])^2 \quad (\text{I})$$

where  $K_{\text{HO}_2} = 1.6 \times 10^{-5} \text{ M}^{-1}$  as recommended values.<sup>14</sup> Reactions 1 and 2 are

$$-\frac{d[\text{HO}_2\cdot/\text{O}_2^{\cdot-}]}{dt} = k_{\text{obs}}[\text{HO}_2\cdot/\text{O}_2^{\cdot-}]^2 \quad (\text{II})$$

The solution of equation (II) is

$$\begin{aligned} k_{\text{obs}} \times t &= \frac{[\text{HO}_2\cdot/\text{O}_2^{\cdot-}]_o}{[\text{HO}_2\cdot/\text{O}_2^{\cdot-}]_o} - \frac{[\text{HO}_2\cdot/\text{O}_2^{\cdot-}]_t}{[\text{HO}_2\cdot/\text{O}_2^{\cdot-}]_t} \\ &\equiv \text{SR} = \frac{A_o - A_t}{A_o A_t} \end{aligned} \quad (\text{III})$$

The signal ratio (SR) can be defined as  $(A_o - A_t)/(A_o \times A_t)$  where  $A_o$  is the CL intensity for a KTR of 0 m, and  $A_t$  is the CL intensity for a KTR of 1 m, 2 m, 3 m, and 4 m, respectively. The CL intensity corresponding to the concentration of  $\text{HO}_2\cdot/\text{O}_2^{\cdot-}$  decreases with increasing lengths of a KTR. A plot of SR vs. KTR yields a straight line. From the slope and intercept of this line, we derive  $\text{KTR}_{t_{1/2}}$  (= the length of the KTR at  $t_{1/2}$ ) from the following equation (IV):

$$\text{SR}_{t_{1/2}} = \text{Slope} \times \text{KTR}_{t_{1/2}} \times \text{Intercept} \quad (\text{IV})$$

where  $\text{SR}_{t_{1/2}}$  is identical with  $1/A_o$  at  $t_{1/2}$ . From the  $\text{KTR}_{t_{1/2}}$  and the constant flow rate for KTR, we derive  $t_{1/2}$ . Since  $[\text{HO}_2\cdot/\text{O}_2^{\cdot-}]_{t_{1/2}}$  is equal to  $[\text{HO}_2\cdot/\text{O}_2^{\cdot-}]_o/2$  at  $t_{1/2}$ , equation (III) becomes

$$[\text{HO}_2\cdot/\text{O}_2^{\cdot-}]_o = \frac{1}{k_{\text{obs}} \times t_{1/2}} \quad (\text{V})$$

Thus, a given concentration of  $\text{HO}_2\cdot/\text{O}_2^{\cdot-}$  can be readily calculated from the equation (V), based on the measured  $t_{1/2}$  and the calculated  $k_{\text{obs}}$  at a given pH.

Figure 4 shows the SR of MCLA-based CL intensity in a CL detector as a function of KTR length at different pH values. In this experiment, the pH levels of a carrier solution were limited to a range of 5.6 (pure water only) to 9.0

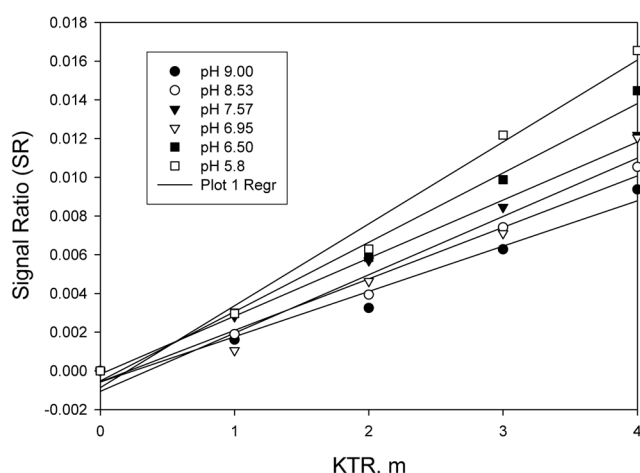


**Figure 4.** Linear plot of signal ratio (SR) versus knotted tubing reactor (KTR) with straight line:  $[\text{MCLA}] = 12 \mu\text{M}$ ,  $[\text{DO}] = 0.094 \text{ mM}$ ,  $\lambda = 254 \text{ nm}$ , and  $\text{pH} = 5.80$ .

(borate buffer). The linear relationship between SR and KTR provides a slope and intercept to experimentally determine  $t_{1/2}$  of  $\text{HO}_2\cdot/\text{O}_2^{\cdot-}$  at a given pH. The SR is proportional to the length of the KTR, which means that the intensity of an MCLA-based CL corresponding to the concentration of  $\text{HO}_2\cdot/\text{O}_2^{\cdot-}$  decreases with an increasing KTR length.

The values for  $\text{SR}_{t_{1/2}}$ ,  $D_{t_{1/2}}$ , half-life ( $t_{1/2}$ ),  $k_{\text{obs}}$ , and concentration of  $\text{HO}_2\cdot/\text{O}_2^{\cdot-}$  at given pH levels are listed in Table 1. The  $t_{1/2}$  and concentration of  $\text{HO}_2\cdot/\text{O}_2^{\cdot-}$  increases as pH increases. These results were due to the  $k_{\text{obs}}$  values on the disproportionation reactions (reactions 6-8) and the pH dependences of the equilibrium between  $\text{HO}_2\cdot$  and  $\text{O}_2^{\cdot-}$ . The pH dependence of  $\text{HO}_2\cdot/\text{O}_2^{\cdot-}$  concentration is distinguished from the different disproportionative reactivities between  $\text{HO}_2\cdot$  and  $\text{O}_2^{\cdot-}$ . Based on  $\text{p}K_a(\text{HO}_2\cdot) = 4.8$ ,<sup>14</sup> the pH dependence of  $\text{HO}_2\cdot/\text{O}_2^{\cdot-}$  refers to the proper apportionment of  $\text{HO}_2\cdot$  and  $\text{O}_2^{\cdot-}$  depending on pH values. For example, the percentages of  $\text{HO}_2\cdot$  and  $\text{O}_2^{\cdot-}$  at pH 5.8 are approximately 9% and 91%, respectively. At pH 9.0 their percentages are approximately 0.01% and 99.99%, respectively. At lower pH condition  $[\text{HO}_2\cdot]/[\text{O}_2^{\cdot-}]$  ratio is relatively high and  $\text{HO}_2\cdot$  reacts relatively fast with  $\text{O}_2^{\cdot-}$  ( $k_{\text{obs}} = 9.51 \times 10^6 \text{ M}^{-1} \text{ s}^{-1}$  at pH 5.8; see Table 1). On the other hand, as the pH increases,

**Table 1.** Summary of the results for the kinetic method in the determination of  $\text{HO}_2\cdot$  on increasing of pH:  $[\text{MCLA}] = 12 \mu\text{M}$ ,  $[\text{DO}] = 0.094 \text{ mM}$ , and  $\lambda = 254 \text{ nm}$ .

pH	$\text{SR}_{t_{1/2}}^a$	$\text{KTR}_{t_{1/2}}^b$ , m	$t_{1/2}$ , seconds	$k_{\text{obs}}^c$ , $\text{M}^{-1} \text{ s}^{-1}$	Concentration of $\text{HO}_2\cdot/\text{O}_2^{\cdot-}$ , M
9.00	11.90	5.33	207.20	$6.00 \times 10^3$	$8.04 \times 10^{-7}$
8.53	12.20	4.39	170.58	$1.77 \times 10^4$	$3.31 \times 10^{-7}$
7.57	12.82	3.96	153.90	$1.61 \times 10^5$	$4.02 \times 10^{-8}$
6.95	11.76	3.90	151.63	$6.73 \times 10^5$	$9.80 \times 10^{-9}$
6.50	10.53	2.97	115.56	$1.90 \times 10^6$	$4.56 \times 10^{-9}$
5.8 <sup>d</sup>	9.09	2.24	87.00	$9.51 \times 10^6$	$1.21 \times 10^{-9}$

<sup>a</sup> $1/A_o$ , where  $A_o$  is the CL intensity at KTR of 0 m. <sup>b</sup>Eq (IV). <sup>c</sup>Eq (I). <sup>d</sup>Pure deionized water only.

$[\text{HO}_2]/[\text{O}_2^{\cdot-}]$  ratio rapidly decreases and the reaction 8 between  $\text{O}_2^{\cdot-}$  and  $\text{O}_2^{\cdot-}$  is dominant and relatively slow ( $k_{\text{obs}} = 6.00 \times 10^3 \text{ M}^{-1}\text{s}^{-1}$  at pH 9.0; see Table 1). Hence, the concentration of  $\text{HO}_2/\text{O}_2^{\cdot-}$  in a basic condition is much more than its concentration in an acidic condition. Therefore, the concentration of  $\text{HO}_2/\text{O}_2^{\cdot-}$  is increased as pH increases. These results are consistent with the kinetic data by Bielski *et al.*<sup>14</sup>

**Comparison of Calibration Techniques.** Because of a new viewpoint on the calibration standard of  $\text{HO}_2/\text{O}_2^{\cdot-}$  generated by the UV photolysis of immobilized  $\text{TiO}_2$ , it is critical to evaluate whether the present method is reliable or not. Under the same experimental condition using a constant flow rate of pure deionized water, the initial concentrations of  $\text{HO}_2/\text{O}_2^{\cdot-}$  were analyzed simultaneously by the present MCLA-CL method and the previous Fenton-like method.<sup>15</sup> The initial concentration ( $1.21 \pm 0.15 \times 10^{-9} \text{ M}$ ) of  $\text{HO}_2/\text{O}_2^{\cdot-}$  determined by the MCLA-CL method was much more with 17% than its concentration ( $1.01 \pm 0.53 \times 10^{-9} \text{ M}$ ) determined by the Fenton-like method. This comparison showing considerable agreement clearly indicates the utility of the MCLA-CL method for measurement of  $\text{HO}_2/\text{O}_2^{\cdot-}$  as a standard.

### Conclusion

We have investigated an in-situ calibration method for the measurement of  $\text{HO}_2/\text{O}_2^{\cdot-}$  using a wet technique. This method was based on the immobilized  $\text{TiO}_2$  photocatalyst and MCLA-based CL technique.  $\text{HO}_2/\text{O}_2^{\cdot-}$  is generated by the UV photolysis of immobilized  $\text{TiO}_2$  using a constant flow rate of air equilibrated water. The concentration of  $\text{HO}_2/\text{O}_2^{\cdot-}$  is readily determined from on the half-life of  $\text{HO}_2^{\cdot}$  and its empirically observed pH-dependent rate constant ( $k_{\text{obs}}$ ) at a given pH. The concentration of  $\text{HO}_2/\text{O}_2^{\cdot-}$  is increased as pH increases. This pH dependence is due to the different disproportionative reactivities between  $\text{HO}_2^{\cdot}$  and  $\text{O}_2^{\cdot-}$ . The concentrations of  $\text{HO}_2/\text{O}_2^{\cdot-}$  are in the range of 1.21 nM (pH 5.80) to 804 nM (pH 9.00).

**Acknowledgements.** This subject is supported by Korea Ministry of Environment as "The Eco-technopia 21 project."

### References

1. Cantrell, C. A.; Stedman, D. H. *Geophys. Res. Lett.* **1982**, *9*, 846-849.
2. Hastie, D. R.; Weissenmayer, M.; Burrows, J. P.; Harris, G. W. *Anal. Chem.* **1991**, *63*, 2048-2057.
3. Lightfoot, R. D.; Cox, R. A.; Crowley, J. N.; Destriau, M.; Hayman, G. D.; Jenkin, M. E.; Moortgat, G. K.; Zabel, F. *Atmospheric Environment*. **1992**, *26A*, 1805-1961.
4. Faust, B. C.; Allen, J. M. *J. Geophys. Res.* **1992**, *97*, 12913-12926.
5. Stevens, P. S.; Mather, J. H.; Brune, W. H. *J. Geophys. Res.* **1994**, *99*, 3543-3557.
6. Hu, J.; Stedman, D. H. *Environ. Sci. Technol.* **1995**, *29*, 1655-1659.
7. Cantrell, C. A.; Shetter, R. E.; Calvert, J. G. *Anal. Chem.* **1996**, *68*, 4194-4199.
8. Kirchner, F.; Stockwell, W. R. *J. Geophys. Res.* **1996**, *101*, 21007-21022.
9. Sillman, S.; He, D.; Pippin, M. R.; Daum, P. H.; Imre, D. G.; Kleinman, L. I.; Lee, J. H.; Weinstein-Lloyd, J. *J. Geophys. Res.* **1998**, *103*, 22629-22644.
10. Zheng, J.; Springston, S. R.; Weinstein-Lloyd, J. *Anal. Chem.* **2003**, *75*, 4696-4700.
11. Heard, D. E.; Pilling, M. J. *Chem. Rev.* **2003**, *103*, 5163-5198.
12. Hard, T. M.; O'Brien, R. J.; Chan, C. Y.; Mehrabzadeh, A. A. *Environ. Sci. Technol.* **1984**, *18*, 768-777.
13. National Aeronautics and Space Administration (NASA). *Assessment of techniques for measuring tropospheric  $\text{H}_2\text{O}_2$* . (Conference Publication 2332); Hoell, J. M., Ed.; Proceeding of a workshop held in Palo Alto; California August 16-20; 1984.
14. Bielski, B. H. J.; Cabelli, D. E.; Arudi, R. L.; Ross, A. B. *J. Phys. Chem. Ref. Data* **1985**, *14*.
15. Kwon, B. G.; Lee, J. H. *Anal. Chem.* **2004**, *76*, 6359-6364.
16. Zhu, Y.; Zhang, L.; Gao, C.; Cao, L. *J. Mater. Sci.* **2000**, *35*, 4049-4054.
17. Courbon, H.; Formenti, M.; Pichat, P. *J. Phys. Chem.* **1977**, *81*, 550-554.
18. Howe, R. F.; Grätzel, M. *J. Phys. Chem.* **1987**, *91*, 3906-3909.
19. Gerisher, H.; Heller, A. *J. Phys. Chem.* **1991**, *95*, 5261-5267.
20. Wang, C.-M.; Heller, A.; Gerischer, H. *J. Am. Chem. Soc.* **1992**, *114*, 5230-5234.
21. Upadhyaya, S.; Ollis, D. F. *J. Phys. Chem. B* **1997**, *101*, 2625-2631.
22. Mills, A.; Hunte, S. L. *Journal of Photochemistry and Photobiology A: Chemistry*. **1997**, *108*, 1-35.
23. Linsebigler, A. L.; Lu, G.; Yates, J. T. Jr. *Chem. Rev.* **1995**, *95*, 735-758.
24. Hoffmann, M. R.; Martin, S. T.; Choi, W.; Bahnemann, D. W. *Chem. Rev.* **1995**, *95*, 69-96.
25. Nosaka, Y.; Yamashita, Y.; Fukuyama, H. *J. Phys. Chem. B* **1997**, *101*, 5822-5827.
26. Hirakawa, T.; Kominami, H.; Ohtani, B.; Nosaka, Y. *J. Phys. Chem. B* **2001**, *105*, 6993-6999.
27. Hirakawa, T.; Nosaka, Y. *Langmuir* **2002**, *18*, 3247-3254.
28. Nakano, M.; Sugioka, K.; Ushijima, Y.; Goto, T. *Anal. Biochem.* **1986**, *159*, 363-369.
29. Shimomura, O.; Wu, C.; Murai, A.; Nakamura, H. *Anal. Biochem.* **1998**, *258*, 230-235.
30. Teranishi, K.; Shimomura, O. *Anal. Biochem.* **1997**, *249*, 37-43.